Transp Porous Med (2010) 81:261–275
DOI 10.1007/s11242-009-9399-9

Slow Motion of an Assemblage of Porous Spherical Shells Relative to a Fluid

Martin P. Keh · Huan J. Keh

Received: 5 July 2008 / Accepted: 10 April 2009 / Published online: 6 May 2009

Abstract The body-force-driven motion of a homogeneous distribution of spherically symmetric porous shells in an incompressible Newtonian fluid and the fluid flow through a bed of these shell particles are investigated analytically. The effect of the hydrodynamic interaction among the porous shell particles is taken into account by employing a cell-model representation. In the limit of small Reynolds number, the Stokes and Brinkman equations are solved for the flow field around a single particle in a unit cell, and the drag force acting on the particle by the fluid is obtained in closed forms. For a suspension of porous spherical shells, the mobility of the particles decreases or the hydrodynamic interaction among the particles increases monotonically with a decrease in the permeability of the porous shells. The effect of particle interactions on the creeping motion of porous spherical shells relative to a fluid can be quite significant in some situations. In the limiting cases, the analytical solution describing the drag force or mobility for a suspension of porous spherical shells reduces to those for suspensions of impermeable solid spheres and of porous spheres. The particle-interaction behavior for a suspension of porous spherical shells with a relatively low permeability may be approximated by that of permeable spheres when the porous shells are sufficiently thick.

Keywords Porous spherical shell · Particle interaction · Creeping flow · Unit cell model · Sedimentation

1 Introduction

The area of the movement of colloidal particles in a fluid at low Reynolds numbers has continued to receive much attention from researchers in the fields of chemical, biomedical, and environmental engineering and science. The majority of these moving phenomena are

M. P. Keh · H. J. Keh (✉)
Department of Chemical Engineering, National Taiwan University, 10617 Taipei, Taiwan, Republic of China
e-mail: huan@ntu.edu.tw

fundamental in nature, but permit one to develop rational understanding of many practical systems and industrial processes such as sedimentation, flotation, agglomeration, spray drying, electrophoresis, and motion of cells in a blood vessel. The theoretical study of this subject has grown out of the classic work of Stokes (1851) for the creeping motion of a rigid sphere in an unbounded viscous fluid and was summarized by Happel and Brenner (1983) among many others.

Being good models for polymer coils in a solvent and for flocs of fine particles in a colloidal suspension, porous particles moving permeably relative to a fluid have also been studied for a long time. A well-known approach which includes a second-order viscous term to Darcy's law for the fluid flow in porous media was developed by Brinkman (1947). Sutherland and Tan (1970) used the Darcy equation for the inside flow field and the Stokes equations for the outside field of a settling porous sphere and concluded that it is reasonable for an isolated sphere on the assumption of immobilized fluid within the porous structure. Their result was proven incorrect by Ooms et al. (1970) and Neale et al. (1973), who used the Brinkman equation for the flow within the porous sphere and more general boundary conditions at the surface of the particle. Experimental studies on the sedimentation of porous particles have been reported by Matsumoto and Suganuma (1977) and Masliyah and Polikar (1980) whose results are in good agreement with the analytical prediction from using the Brinkman equation.

The low-Reynolds-number flow of an incompressible Newtonian fluid past a spherical composite particle having a central solid core and an outer porous shell was solved by Masliyah et al. (1987) and Veerapaneni and Wiesner (1996) using the Brinkman and Stokes equations. An analytical formula for the hydrodynamic drag force experienced by the particle was derived as a function of the radius of the solid core, the thickness of the porous shell, and the permeability of the shell. Masliyah et al. also measured the settling velocity of a solid sphere with attached threads and found that theoretical predictions for the composite sphere are in excellent agreement with the experimental results. Recently, the motion of a composite sphere situated at the center of a spherical cavity was analyzed by Keh and Chou (2004) and Srinivasacharya (2005).

On the other hand, Jones (1973) analyzed the creeping motion of a spherically symmetric porous shell using Darcy's law and an empirical boundary condition. Later on, the same problem was investigated by Qin and Kaloni (1993) and Bhatt and Sacheti (1994) using the Brinkman equation and well-defined boundary conditions at the surfaces of the porous shell. There were several features in their analytical solutions, which cannot be seen from Darcy's solution. When the internal surface of the porous spherical shell shrinks to the limit, the particle reduces to a permeable sphere. Recently, the translational and rotational motions of a porous spherical shell in a concentric spherical cavity have been studied analytically by Keh and Lu (2005).

In practical applications of particle motion relative to a fluid, collections of particles are usually encountered. Thus, it is important to determine whether the presence of neighboring particles significantly affects the movement of an individual particle. A method which has been employed successfully to predict the effect of particle concentration on the particle sedimentation rate is the unit cell model (Happel and Brenner 1983; Prasad et al. 1990). This model involves the concept that an assemblage of spherical particles can be divided into a number of identical cells, one particle occupying each cell. The boundary-value problem for multiple spheres is thus reduced to the consideration of the behavior of a single sphere and its bounding envelope. Although different shapes of cells can be chosen, the assumption of a spherical shape for the fictitious envelope of fluid surrounding each spherical particle is

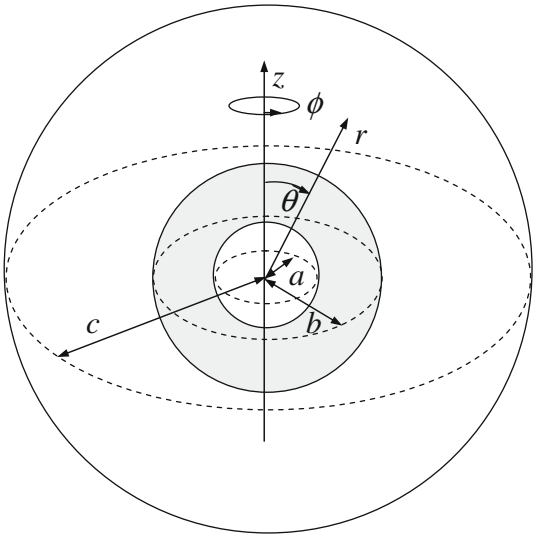

Fig. 1 Geometrical sketch for the relative motion of a porous spherical shell at the center of a spherical cell

of great convenience. The cell model is of great applicability in concentrated assemblages, where the effect of container walls will not be important.

In this study, the unit cell model is used to study the hydrodynamic interaction among a swarm of identical, spherically symmetric, porous shells with an arbitrary shell thickness moving relative to a fluid. The solutions obtained with this model enable the sedimentation rate in a suspension of porous spherical shells or alternatively the pressure drop for a fluid flow through a bed of porous spherical shells to be predicted as a function of the microstructure and volume fraction of the porous shell particles. In the limit of zero volume fraction of the particles, our result reduces to that obtained by Qin and Kaloni (1993) and Bhatt and Sacheti (1994) for the motion of an isolated porous spherical shell in the absence of the other ones.

2 Analysis

Consider the steady body-force-driven motion (e.g., sedimentation) of a uniform distribution of identical, spherically symmetric, porous shells of external radius b and internal radius a in an incompressible Newtonian fluid of viscosity η. In each fluid-permeable porous shell, idealized hydrodynamic frictional segments are assumed to distribute uniformly. The porous shell particles are taken to be non-deformable, and their average migration velocity equals U in the positive z direction. As shown in Fig. 1, we employ a unit cell model in which each porous shell particle is surrounded by a concentric spherical envelope of suspending fluid having an outer radius c such that the ratio of the particle volume (taken as $4\pi b^3/3$) to the cell volume is equal to the particle volume fraction φ throughout the entire suspension; viz., $\varphi = (b/c)^3$. The origin of the spherical coordinate system (r, θ, ϕ) is set at the particle or cell center. The Reynolds number is assumed to be sufficiently small so that the inertial terms in the fluid momentum equation can be neglected, in comparison with the viscous terms. Our objective is to determine the hydrodynamic drag force exerted on the porous shell particle moving with the velocity U in a unit cell.

The external region ($b \leq r \leq c$), porous region ($a \leq r \leq b$), and internal region ($r \leq a$) in a cell are denoted by regions I, II, and III, respectively. Then, the fluid flow in regions I and III is governed by the Stokes equations

$$\eta \nabla^2 \mathbf{v}_i - \nabla p_i = \mathbf{0}, \tag{1a}$$

$$\nabla \cdot \mathbf{v}_i = 0. \tag{1b}$$

Here, $\mathbf{v}$ is the velocity field for the fluid flow relative to the porous shell, p is the corresponding dynamic pressure distribution, $i = 1$ or 3, and the subscripts 1 and 3 represent the regions I and III, respectively.

For the fluid flow within the porous shell, the relative velocity $\mathbf{v}_2$ and dynamic pressure p_2 (where subscript 2 represents macroscopically averaged quantities pertaining to region II) are governed by the Brinkman equation

$$\eta \nabla^2 \mathbf{v}_2 - \frac{\eta}{k} \mathbf{v}_2 - \nabla p_2 = \mathbf{0} \tag{2a}$$

and the continuity equation

$$\nabla \cdot \mathbf{v}_2 = 0, \tag{2b}$$

where k is the permeability of the porous shell. For some model porous particles made of steel wool (Matsumoto and Suganuma 1977) and plastic foam slab (Masliyah and Polikar 1980), the experimental values of k can be as large as $10^{-7}\,\mathrm{m}^2$, while in the poly(N-isopropylacrylamide) hydrogel layers on latex particles, values of k were found to be about 10^{-15}–$10^{-18}\,\mathrm{m}^2$ (Makino et al. 1994). In Eq. 2a, we have assumed that the fluid has the same viscosity inside and outside the permeable shell which is reasonable according to the available evidence (Koplik et al. 1983).

The fluid-flow field in a cell is axially symmetric; thus, it is convenient to introduce the Stokes stream functions $\psi_i(r, \theta)$ which satisfy Eqs. 1b and 2b and are related to the velocity components in the spherical coordinate system by

$$v_{ri} = -\frac{1}{r^2 \sin\theta} \frac{\partial \psi_i}{\partial \theta}, \tag{3a}$$

$$v_{\theta i} = \frac{1}{r \sin\theta} \frac{\partial \psi_i}{\partial r}. \tag{3b}$$

Taking the curl of Eq. 1a and applying Eq. 3, one obtains a fourth-order linear partial differential equation for ψ_i (Happel and Brenner 1983),

$$E_s^2 (E_s^2 \psi_i) = 0, \tag{4}$$

where $i = 1$ or 3, and the Stokes operator E_s^2 is given by

$$E_s^2 = \frac{\partial^2}{\partial r^2} + \frac{\sin\theta}{r^2} \frac{\partial}{\partial \theta} \left(\frac{1}{\sin\theta} \frac{\partial}{\partial \theta} \right). \tag{5}$$

Similarly, Eq. 2a can be expressed in terms of the stream function $\psi_2(r, \theta)$ as

$$E_s^2 \left(E_s^2 \psi_2 - \frac{1}{k} \psi_2 \right) = 0. \tag{6}$$

Owing to the continuity of velocity and stress components at the surface of a porous medium, which is physically realistic and mathematically consistent for the present problem

(Neale et al. 1973; Chen and Cai 1999; Keh and Chen 2006), the boundary conditions for the flow field at the surfaces of the porous shell are

$$r = a: \ v_{r3} = v_{r2}, \ v_{\theta 3} = v_{\theta 2}, \tag{7a,b}$$

$$\tau_{rr3} = \tau_{rr2}, \ \tau_{r\theta 3} = \tau_{r\theta 2}; \tag{8a,b}$$

$$r = b: \ v_{r2} = v_{r1}, \ v_{\theta 2} = v_{\theta 1}, \tag{9a,b}$$

$$\tau_{rr2} = \tau_{rr1}, \ \tau_{r\theta 2} = \tau_{r\theta 1}. \tag{10a,b}$$

In Eqs. 8 and 10, τ_{rr} and $\tau_{r\theta}$ are the normal and shear stresses for the fluid flow relevant to the particle surfaces.

On the outer (virtual) boundary of the unit cell, the Happel model assumes that the radial velocity and the shear stress of the fluid are zero (Happel 1958), viz,

$$r = c: \ v_{r1} = -U\cos\theta, \tag{11a}$$

$$\tau_{r\theta 1} = 0. \tag{11b}$$

Clearly, in this model, the outer edge of the cell is taken to be a free surface. Equations 7–11 take a reference frame that the porous spherical shell is at rest, and the radial velocity of the fluid at the outer boundary of the cell is that of the particle in the opposite direction.

A sufficiently general solution to Eqs. 4 and 6 suitable for satisfying boundary conditions on the spherical surfaces is (Masliyah et al. 1987; Keh and Lu 2005)

$$\psi_1 = \frac{1}{2}kU\left(A\xi^{-1} + B\xi + C_1\xi^2 + D_1\xi^4\right)\sin^2\theta \quad \text{if } \beta \le \xi \le \gamma, \tag{12a}$$

$$\psi_2 = \frac{1}{2}kU\left[E\xi^{-1} + F\xi^2 + G\left(\xi^{-1}\cosh\xi - \sinh\xi\right) + H\left(\xi^{-1}\sinh\xi - \cosh\xi\right)\right]\sin^2\theta \quad \text{if } \alpha \le \xi \le \beta, \tag{12b}$$

$$\psi_3 = \frac{1}{2}kU\left(C_3\xi^2 + D_3\xi^4\right)\sin^2\theta \quad \text{if } \xi \le \alpha, \tag{12c}$$

where the dimensionless variables $\xi = r/k^{1/2}$, $\alpha = a/k^{1/2}$, $\beta = b/k^{1/2}$, and $\gamma = c/k^{1/2}$. The dimensionless constants A, B, C_1, D_1, C_3, D_3, E, F, G, and H are found from Eqs. 7–11 using Eq. 3, and the result is presented in Appendix A.

The drag force (in the z direction) acting on the porous spherical shell by the external fluid can be determined from (Happel and Brenner 1983)

$$F_{\mathrm{d}} = 4\pi\eta k^{1/2} U B, \tag{13}$$

where B is given by Eq. A-12 in Appendix A.

In the limit $\beta/\gamma = b/c = 0$, Eq. 13 becomes

$$F_{\mathrm{d}}^{(0)} = -6\pi\eta b U \frac{R}{\beta S}, \tag{14}$$

where

$$R = 2\left(3\beta w_2 - \alpha w_1\right)\cosh\left(\beta - \alpha\right) - 2\left(3w_2 - \alpha\beta w_1\right)\sinh\left(\beta - \alpha\right), \tag{15a}$$

$$S = 60\alpha^3 - 3\left[\left(\alpha^2+15\right)\left(4\alpha^3+\alpha-w_3\right) - \alpha^2 w_3 - 10\alpha\left(5\alpha^2-3\right)\right]\cosh(\beta-\alpha) - \left[\left(\alpha^2+15\right)\left(2\alpha^4+9-\alpha w_3\right) - 30\alpha w_3 + 9\alpha^2\right]\sinh(\beta-\alpha) \tag{15b}$$

with

$$w_1 = \beta^3\left(\alpha^2+45\right) - \alpha^3\left(\alpha^2+15\right), \tag{16a}$$

$$w_2 = \beta^3\left(2\alpha^2+15\right) - \alpha^3\left(2\alpha^2+5\right), \tag{16b}$$

$$w_3 = \beta\left(2\beta^2+3\right). \tag{16c}$$

Equations 14–16 are the same as the result obtained by Bhatt and Sacheti (1994) for the motion of an isolated porous spherical shell in the absence of the other ones.

In terms of Eqs. 13 and 14, the normalized mobility of the porous spherical shell in a unit cell can be expressed as

$$M = \frac{F_{\mathrm{d}}^{(0)}}{F_{\mathrm{d}}} = -\frac{3R}{2BS}, \tag{17}$$

which leads to $M = 1$ as $\beta/\gamma = \varphi^{1/3} = 0$ and $0 \le M < 1$ as $0 < \beta/\gamma \le 1$. The presence of the virtual surface of the unit cell always enhances the hydrodynamic drag on the particle since the radial fluid flow vanishes there as required by Eq. 11a.

In the limiting case of $k = 0$, $F_{\mathrm{d}}^{(0)} = -6\pi\eta bU$, (Stokes' law) and Eq. 17 reduces to

$$M = \left(1 - \frac{3}{2}\varphi^{1/3} + \frac{3}{2}\varphi^{5/3} - \varphi^2\right)\left(1 + \frac{2}{3}\varphi^{5/3}\right)^{-1}, \tag{18}$$

where $\varphi = (b/c)^3$. This is the result for the motion of an impermeable solid sphere of radius b in a cell of radius c.

In the limit $a = 0$, Eqs. 14 and 17 become

$$F_{\mathrm{d}}^{(0)} = -6\pi\eta bU\frac{2\beta^2(\beta-\tanh\beta)}{2\beta^3+3(\beta-\tanh\beta)}, \tag{19}$$

$$M = 3(\beta-\tanh\beta)\left\{\beta\left[3\left(s_8-10\beta^5\right) + \beta^2\left(2s_8-25\beta^5\right) - 30\beta^5 - \beta^2 s_2\varphi^{\frac{1}{3}}\right] - 3\left[s_8+5\beta^7+10\beta^5-\beta^2 s_1\varphi^{\frac{1}{3}}\right]\tanh\beta\right\} \times\left[\beta s_2 - 3s_1\tanh\beta\right]^{-1}\times\left[\beta\left(2\beta^2+3\right) - 3\tanh\beta\right]^{-1}, \tag{20}$$

where the dimensionless parameters s_1, s_2, and s_8 are defined by Eq. A-22. The hydrodynamic drag force and normalized mobility given by Eqs. 19 and 20 describe the motion of a porous (permeable) sphere of radius b in an unbounded fluid (Neale et al. 1973) and in a cell of radius c, respectively.

The results of the mean particle mobility in a suspension can also be applied to the case of a fluid flow through a bed of particles. For the model under consideration, the drag force F_{d} divided by the cell volume $4\pi c^3/3$ will equal $-\Delta P/L$, the pressure drop per unit length of bed due to the passage of fluid through it. The usage of this relationship and Eq. 13 gives the superficial fluid velocity through a bed of porous spherical shells as

$$U = \left(-\frac{\beta b^2}{3B\varphi}\right)\frac{\Delta P}{\eta L}, \tag{21}$$

where the quantity in parentheses is the permeability coefficient in Darcy's law for the whole bed. If we use $U^{(0)}$ and $\Delta P^{(0)}$ to represent U and ΔP, respectively, in the limit of $\varphi \to 0$ (a loose bed), the ratio $U/U^{(0)}$ with $\Delta P = \Delta P^{(0)}$ (equals the ratio $\Delta P^{(0)}/\Delta P$ with $U = U^{(0)}$) is also equal to the normalized mobility M given by Eq. 17.

When the Kuwabara model for the boundary condition of the fluid flow at the virtual surface of the unit cell, which assumes that the radial velocity and the vorticity are zero (Kuwabara 1959), is used, Eq. 11b is replaced by

$$r = c: \ (\nabla \times \mathbf{v})_\phi = \frac{\partial v_\theta}{\partial r} + \frac{v_\theta}{r} - \frac{1}{r}\frac{\partial v_r}{\partial \theta} = 0. \tag{22}$$

With this change, the stream functions ψ_i and the drag force F_d can still be expressed in the forms of Eqs. 12 and 13, but the coefficients A, B, C_1, D_1, C_3, D_3, E, F, G, and H should be determined by boundary conditions 7–10, 11a, and 22. The results of these coefficients are given in Appendix A, in which B is given by Eq. A-25. It has been shown that the Kuwabara cell model can be quite satisfactory for the analysis of phoretic motions of suspensions of identical colloidal particles, where the fluid flow around a phoretic particle is irrotational and vorticity free (Wei and Keh 2001).

It is easy to find that for the case of the Kuwabara model, Eq. 18 in the limit of $k = 0$ and Eq. 20 in the limit of $a = 0$ for the normalized particle mobility become

$$M = 1 - \frac{9}{5}\varphi^{\frac{1}{3}} + \varphi - \frac{1}{5}\varphi^2 \tag{23}$$

and

$$\begin{aligned} M = \frac{1}{5\beta^3}\Big\{\beta\Big[\beta^2\left(6\beta^3 + 30\beta - 2t_3\right)\varphi^2 + 15\left(t_1 + 8\beta^3\right)\varphi + 2\beta^4\left(5\gamma - 9\beta\right)\varphi^{\frac{1}{3}}\Big] \\ - \Big[6\beta^2\left(85\beta - t_2\right)\varphi^2 + 15\left(t_1 + 8\beta^3\right)\varphi - 18\beta^5\varphi^{\frac{1}{3}}\Big]\tanh\beta\Big\} \\ \times\left[\beta\left(2\beta^2 + 3\right) - 3\tanh\beta\right]^{-1}, \end{aligned} \tag{24}$$

respectively. In Eq. 24, the dimensionless parameters t_1, t_2, and t_3 are given by Eq. A-35. It can be seen in Eqs. 18 and 23 that the leading order of the particle concentration effect on the particle mobility is $\varphi^{1/3}$ and this effect predicted by the Kuwabara model is stronger than that for the Happel model.

3 Results and Discussion

Analytical results for the sedimentation of a homogeneous distribution of identical porous spherical shells and the fluid flow through a bed of these particles have been obtained in the previous section using a unit cell model. Figure 2 illustrates the variation of the normalized mobility M for the motion of a suspension of porous spheres (with $a = 0$) given by Eqs. 20 and 24 for the Happel and Kuwabara models, respectively, with the volume fraction φ of the particles for various values of the parameter β. The calculations are presented up to $\varphi = 0.74$, which corresponds to the maximum attainable volume fraction for a swarm of identical spheres (Levine and Neale 1974). The curve with $\beta = 0$ represents the result for porous spheres with no resistance to the fluid flow, whereas the curve with $\beta \to \infty$ denotes the result for impermeable solid spheres. For any specified finite value of β, the normalized mobility M decreases monotonically with an increase in φ.

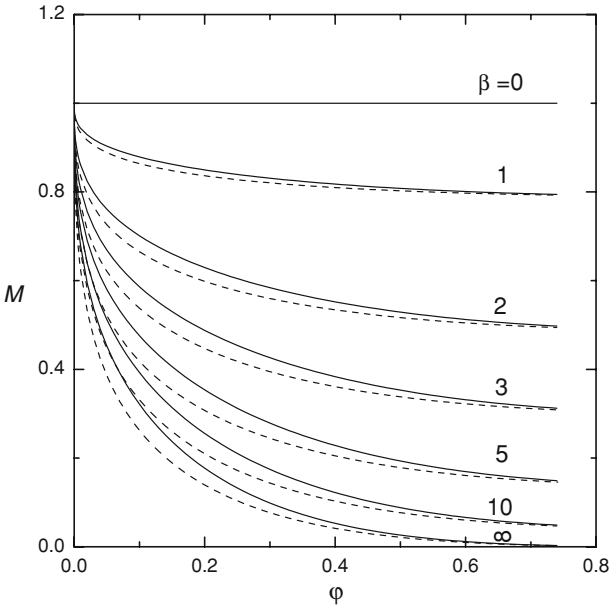

Fig. 2 Plots of the normalized mobility M in a suspension of identical porous spheres $a = 0$ versus the particle volume fraction φ for various values of β. The *solid* and *dashed curves* represent the calculations for the Happel (Eq. 20) and Kuwabara (Eq. 24) cell models, respectively

Figure 2 indicates that the particle interaction effect on the mobility is stronger when the permeability k of the porous particles is smaller (or β is greater). For $\beta < 1$, the particle mobility varies slowly with the volume fraction φ, compared with the case of a greater value of β. For $\beta > 10$, the value of the particle mobility is quite close to that of impermeable solid particles when φ is small, but the difference becomes more significant, as the particles get closer with one another. The physical explanation of this behavior was provided by Keh and Lu (2005). For constant values of β and φ, the Kuwabara model predicts a stronger concentration effect on the particle mobility (or a smaller mean particle mobility) than the Happel model does. This occurs because the zero-vorticity model yields a greater energy dissipation in the cell than that due to particle drag alone, owing to the additional work done by the stresses at the outer boundary (Happel and Brenner 1983). The predictions of the two models, in general, result in the same behavior qualitatively and are in numerical agreement to within 15%.

Chen and Cai (1999) obtained the numerical solution of the hydrodynamic interaction between pairs of settling porous spheres using a boundary collocation method and derived an ensemble-averaged formula for the mean particle mobility in a dilute suspension of identical porous spheres (say, $\varphi < 0.1$) in the form

$$M = 1 - \alpha_1 \varphi + O(\varphi^2). \tag{25}$$

Consistent with the trend shown in Fig. 2, their values of α_1 (which are always positive) increase with an increase in β (e.g., $\alpha_1 = 3.46$ as $\beta = 3.16$ and $\alpha_1 = 6.23$ as $\beta = 31.6$). Note that as the value of φ is small, M varies linearly with φ in Eq. 25, while Eqs. 18, 20, 23, and 24 indicate that M depends linearly with $\varphi^{1/3}$ for the cell model.

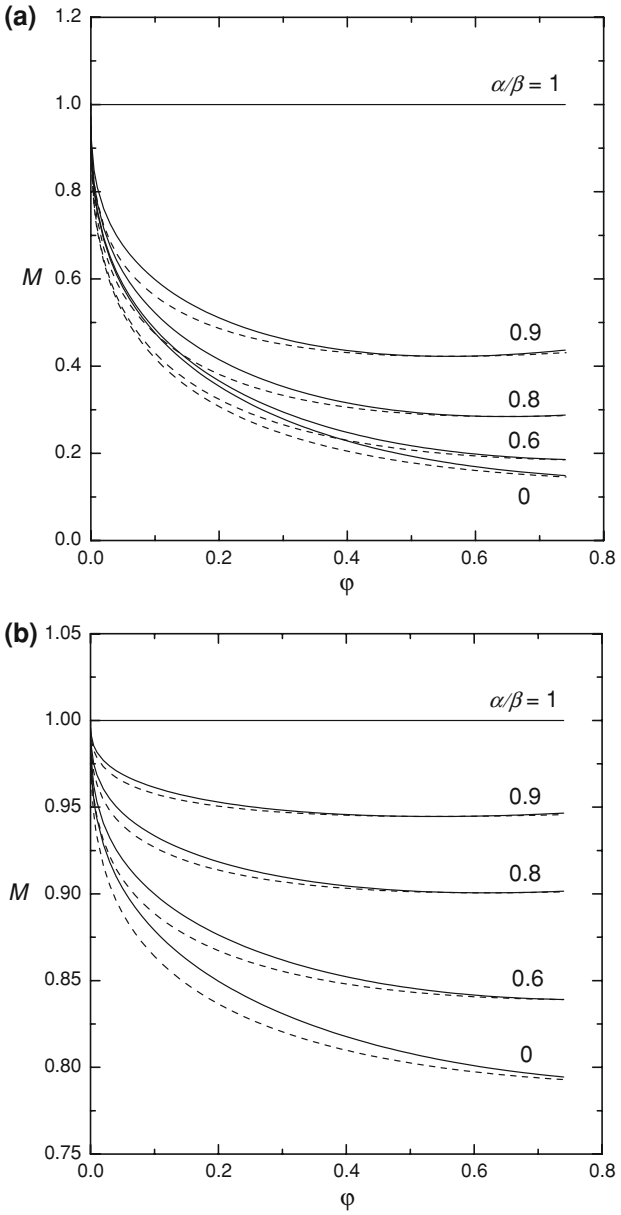

Fig. 3 Plots of the normalized mobility M in a suspension of identical porous spherical shells versus the particle volume fraction φ for various values of α/β: (**a**) $\beta = 5$; (**b**) $\beta = 1$. The *solid* and *dashed* curves represent the calculations for the Happel and Kuwabara cell models, respectively

For the general case of the motion of an assemblage of porous spherical shells, Fig. 3a and b show the normalized mobility M as a function of the volume fraction φ and the parameter α/β over the entire possible range for the cases of $\beta = 5$ and 1, respectively. As expected, in the limit of $\varphi \to 0$, $M = 1$ and the result obtained by Qin and Kaloni (1993) and

Bhatt and Sacheti (1994) for the motion of an isolated porous spherical shell is recovered. In general, M is a decreasing function of φ for fixed values of α/β and β, and is a decreasing function of β for constant values of α/β and φ. M is a monotonic increasing function of α/β for given values of β and φ, and the curves with $\alpha/\beta = 0$ represent the result for porous spheres, which was also given in Fig. 2. Similar to that discussed by Keh and Lu (2005), for the case of $\beta = 5$, the behavior of porous spherical shells with $\alpha/\beta = 0.6$ can be roughly approximated by that of porous spheres of equal size and permeability when $\varphi < 0.2$. However, this approximation is relatively poor for porous shells with a large permeability, as for the case of $\beta = 1$ shown in Fig. 3b.

4 Concluding Remarks

In this study, the slow motion of an assemblage of identical porous spherical shells relative to an incompressible Newtonian fluid is analyzed using the Happel and Kuwabara cell models. In a unit cell, the Brinkman and Stokes equations for the fluid flow field are solved and the hydrodynamic drag force acting on the porous shell particles as a function of the parameters $\alpha/\beta\ (= a/b)$, $\varphi\ \left(= (b/c)^3\right)$, and β is obtained in closed-form expressions. It has been found that the effect of the hydrodynamic interaction among porous spherical shells is weaker than that among porous spheres with the same permeability. For a suspension of porous shell particles with fixed values of α/β and φ, the mobility of each particle normalized by its corresponding value in the absence of the other ones is a monotonic decreasing function of the parameter β (or an increasing function of the permeability k) of the particles. For given values of α/β and β, this normalized mobility, in general, decreases with an increase in the volume fraction φ of the particles.

The results presented in the previous sections indicate that the effect of the hydrodynamic interaction among the porous shell particles in a suspension can be significant in some situations. Both the Happel and the Kuwabara models give essentially the same fluid velocity field and approximately equal particle mobility for the motion of porous spherical shells. However, the Happel model has a significant advantage in that it does not require an exchange of mechanical energy between the cell and the environment (Happel and Brenner 1983). Another unit cell model proposed by Simha (1952) with the assumption that both the normal and the tangential components of the fluid velocity vanish at the outer boundary of the cell is evidently less reasonable than the Happel or Kuwabara model. The relevant experimental data, which are not available in the literature, would be needed to confirm the validity of the cell model at various ranges of the parameters α/β, β, and φ of the suspension of porous shells.

Acknowledgement Part of this research was supported by the National Science Council of the Republic of China.

Appendix A

The algebraic equations for the determination of the coefficients in Eq. 12 as well as their solutions are presented in this appendix. Applying the boundary conditions given by Eqs. 7–11 for the Happel model to the general solution given by Eq. 12 for the motion of a porous spherical shell in a concentric spherical cell, one obtains

$$C_3\alpha^3 + D_3\alpha^5 = E + F\alpha^3 - G\left(\alpha\sinh\alpha - \cosh\alpha\right) + H\left(\sinh\alpha - \alpha\cosh\alpha\right), \quad \text{(A-1)}$$

$$\begin{aligned} -2C_3\alpha^3 - 4D_3\alpha^5 = {} & E - 2F\alpha^3 - G\left[\alpha\sinh\alpha - \left(\alpha^2+1\right)\cosh\alpha\right] \\ & - H\left[\alpha\cosh\alpha - \left(\alpha^2+1\right)\sinh\alpha\right], \end{aligned} \quad \text{(A-2)}$$

$$6D_3\alpha^5 = 6E + 3\left(\alpha^2+2\right)\left(G\cosh\alpha + H\sinh\alpha\right) - \alpha\left(\alpha^2+6\right)\left(G\sinh\alpha + H\cosh\alpha\right), \quad \text{(A-3)}$$

$$20D_3\alpha^3 = E - 2F\alpha^3, \quad \text{(A-4)}$$

$$\begin{aligned} A + B\beta^2 + C_1\beta^3 + D_1\beta^5 = {} & E + F\beta^3 - G\left(\beta\sinh\beta - \cosh\beta\right) \\ & + H\left(\sinh\beta - \beta\cosh\beta\right), \end{aligned} \quad \text{(A-5)}$$

$$\begin{aligned} A - B\beta^2 - 2C_1\beta^3 - 4D_1\beta^5 = {} & E - 2F\beta^3 - G\left[\beta\sinh\beta - \left(\beta^2+1\right)\cosh\beta\right] \\ & - H\left[\beta\cosh\beta - \left(\beta^2+1\right)\sinh\beta\right], \end{aligned} \quad \text{(A-6)}$$

$$\begin{aligned} 6A + 6D_1\beta^5 = {} & 6E + 3\left(\beta^2+2\right)\left(G\cosh\beta + H\sinh\beta\right) \\ & - \beta\left(\beta^2+6\right)\left(G\sinh\beta + H\cosh\beta\right), \end{aligned} \quad \text{(A-7)}$$

$$2B + 20D_1\beta^3 = E - 2F\beta^3, \quad \text{(A-8)}$$

$$A + B\gamma^2 + C_1\gamma^3 + D_1\gamma^5 = \gamma^3, \quad \text{(A-9)}$$

$$A + D_1\gamma^5 = 0. \quad \text{(A-10)}$$

These simultaneous algebraic equations can be solved to yield the 10 unknown constants as

$$A = -\gamma^5 D_1, \quad \text{(A-11)}$$

$$\begin{aligned} B = \Delta\gamma\Big\{ & -600\alpha^3\beta^6 - 3[-45\alpha\beta^3 s_1 + \left(15\alpha^4 + \alpha^6\right)\left(s_1 + 20\beta^3\right) \\ & + 15\beta^4 s_2 - 2\alpha^5 s_3 - \alpha^3\beta s_4 + \alpha^2 s_5]\cosh\left(\beta - \alpha\right) + [\left(135\beta^3 + 18\alpha^2\beta^3\right)s_1 \\ & - 18\alpha^5\left(s_1 + 20\beta^3\right) - 45\alpha\beta^4 s_2 + \left(15\alpha^4 + \alpha^6\right)s_3 - \alpha^3 s_6]\sinh\left(\beta - \alpha\right)\Big\}, \end{aligned} \quad \text{(A-12)}$$

$$C_1 = 1 - B\gamma^{-1}, \quad \text{(A-13)}$$

$$\begin{aligned} C_3 = \Delta 3\gamma\Big\{ & s_7 - 3\left[\left(-15\beta - 7\alpha^2\beta\right)\left(s_1 + 20\beta^3\right) + \left(15\alpha + 2\alpha^3\right)s_8\right]\cosh\left(\beta - \alpha\right) \\ & + 3\left[-\left(15 + 7\alpha^2\right)s_8 + \alpha\beta\left(15 + 2\alpha^2\right)\left(s_1 + 20\beta^3\right)\right]\sinh\left(\beta - \alpha\right)\Big\}, \end{aligned} \quad \text{(A-14)}$$

$$\begin{aligned} D_1 = \Delta\beta^2\gamma\Big\{ & -30\alpha^3\beta - 3\left[\alpha^4\left(15 + \alpha^2 - 2\alpha\beta\right) + \left(15\beta^2 + 2\alpha^2\beta^2\right)\left(6 + \beta^2\right)\right. \\ & - 45\alpha\beta\left(2 + \beta^2\right) - \alpha^3\beta\left(7 + \beta^2\right)\Big]\cosh\left(\beta - \alpha\right) - \Big[45\alpha^3 + \alpha^4\left(18\alpha - 15\beta - \alpha^2\beta\right) \\ & - \left(135\beta + 18\alpha^2\beta\right)\left(2 + \beta^2\right) + \left(45\alpha\beta^2 + \alpha^3\beta\right)\left(6 + \beta^2\right)\Big]\sinh\left(\beta - \alpha\right)\Big\}, \end{aligned} \quad \text{(A-15)}$$

$$D_3 = -\Delta 3\gamma \left\{ s_9 - 3\left[\alpha s_8 - \beta\left(s_8 - 10\beta^5\right)\right]\cosh(\beta-\alpha) + 3\left[\alpha\beta\left(s_8 - 10\beta^5\right) - s_8\right]\sinh(\beta-\alpha)\right\}, \tag{A-16}$$

$$E = -6\Delta\alpha^3\gamma \left\{ 10\beta^3\left(\beta^5 - \gamma^5\right) + \left[\left(-15\beta - 6\alpha^2\beta\right)\left(s_8 - 10\beta^5\right) + \left(15\alpha + a^3\right)s_8\right]\cosh(\beta-\alpha) + \left[3\left(5 + 2\alpha^2\right)s_8 - \alpha\beta\left(15 + \alpha^2\right)\left(s_8 - 10\beta^5\right)\right] \times \sinh(\beta-\alpha)\right\}, \tag{A-17}$$

$$F = \Delta 3\gamma \left\{ 10\alpha^3\left(s_8 - 15\beta^5\right) + \left[\left(45\beta + 6\alpha^2\beta\right)\left(s_8 - 10\beta^5\right) + \left(-45\alpha - \alpha^3\right)s_8\right] \times \cosh(\beta-\alpha) - \left[3\left(15 + 2\alpha^2\right)s_8 - \alpha\beta\left(45 + \alpha^2\right)\left(s_8 - 10\beta^5\right)\right]\sinh(\beta-\alpha)\right\}, \tag{A-18}$$

$$G = \Delta 6\gamma \left\{ \left[\left(45\alpha\beta^3 + \alpha^3\beta^3\right)\left(\beta^5 - \gamma^5\right) + \left(15\alpha^4 + \alpha^6\right)\left(s_8 - 15\beta^5\right)\right]\cosh\alpha - 15\alpha^3\beta\left(s_8 - 10\beta^5\right)\cosh\beta - 3\left[\left(15\beta^3 + 2\alpha^2\beta^3\right)\left(\beta^5 - \gamma^5\right) + \left(5\alpha^3 + 2\alpha^5\right)\left(s_8 - 15\beta^5\right)\right]\sinh\alpha + \left(15\alpha^3 s_8\right)\sinh\beta\right\}, \tag{A-19}$$

$$H = \Delta 6\gamma \left\{ 3\left[\left(15\beta^3 + 2\alpha^2\beta^3\right)\left(\beta^5 - \gamma^5\right) + \left(5\alpha^3 + 2\alpha^5\right)\left(s_8 - 15\beta^5\right)\right]\cosh\alpha - \left(15\alpha^3 s_8\right)\cosh\beta - \left[\left(45\alpha\beta^3 + \alpha^3\beta^3\right)\left(\beta^5 - \gamma^5\right) + \left(15\alpha^4 + \alpha^6\right)\left(s_8 - 15\beta^5\right)\right]\sinh\alpha + 15\alpha^3\beta\left(s_8 - 10\beta^5\right)\sinh\beta\right\}, \tag{A-20}$$

where

$$\Delta = -\left\{ 60\alpha^3\left[10\beta^6 - \gamma\left(s_8 - 5\beta^5\right)\right] + 3\left[\left(15\alpha^4 + \alpha^6\right)\left(s_8 - 10\beta^5 - 5\beta^4\gamma\right) - 2\alpha^5 s_{10} - \alpha^3\left(\beta s_4 - 39\beta^5\gamma - 5\beta^7\gamma - 11\gamma^6 - 330\beta^3\gamma\right) + \left(15\beta + 2\alpha^2\beta\right)s_{11} - 45\alpha s_{12}\right]\cosh(\beta-\alpha) - \left[-18\alpha^5\left(s_8 - 10\beta^5 - 5\beta^4\gamma\right) + \left(15\alpha^4 + \alpha^6\right)s_{10} + \left(135 + 18\alpha^2\right)s_{12} - 45\alpha\beta s_{11} + \alpha^3 s_{13}\right]\sinh(\beta-\alpha)\right\}^{-1}, \tag{A-21}$$

$$\begin{aligned}
s_1 &= 10\beta^3 + 4\beta^5 + \gamma^5, \quad s_2 = 30\beta^3 + 2\beta^5 + 3\gamma^5,\\
s_3 &= 90\beta^4 + 2\beta^6 + 3\beta\gamma^5, \quad s_4 = 450\beta^3 + 20\beta^5 + 4\beta^7 + 15\gamma^5 + \beta^2\gamma^5,\\
s_5 &= 60\beta^7 + 4\beta^9 + 6\beta^4\gamma^5, \quad s_6 = 1350\beta^3 + 180\beta^5 + 30\beta^7 + 2\beta^9 + 45\gamma^5 + 3\beta^4\gamma^5,\\
s_7 &= 30\alpha^5\beta^3 - \alpha^5\beta^5 - 30\beta^8 + \alpha^2\beta^8 + \alpha^5\gamma^5 + 30\beta^3\gamma^5 - \alpha^2\beta^3\gamma^5,\\
s_8 &= 30\beta^3 + 14\beta^5 + \gamma^5, \quad s_9 = 30\alpha^3\beta^3 - \alpha^3\beta^5 + \beta^8 + \alpha^3\gamma^5 - \beta^3\gamma^5,\\
s_{10} &= 90\beta^4 + 2\beta^6 - 60\beta^3\gamma - 3\beta^5\gamma + 3\beta\gamma^5 - 2\gamma^6,\\
s_{11} &= 30\beta^6 + 2\beta^8 - 42\beta^5\gamma - 3\beta^7\gamma - 3\gamma^6 - 2\beta^2\gamma^6 - 90\beta^3\gamma + 3\beta^3\gamma^5,\\
s_{12} &= 10\beta^6 + 4\beta^8 - 24\beta^5\gamma - 5\beta^7\gamma - \gamma^6 - 30\beta^3\gamma + \beta^3\gamma^5,
\end{aligned}$$

$$s_{13} = -180\beta^5 - 30\beta^7 - 2\beta^9 + 42\beta^6\gamma + 3\beta^8\gamma - 45\gamma^5 + 3\beta\gamma^6 - 3\beta^4\gamma\left(-105 + \gamma^4\right) + 2\beta^3\left(-675 + \gamma^6\right). \tag{A-22}$$

If the Kuwabara model is used, one can apply the boundary conditions given by Eqs. 7–10, 11a, and 22 to the general solution given by Eq. 12 to yield Eqs. A1–A9 and

$$B - 5D_1\gamma^3 = 0. \tag{A-23}$$

The simultaneous solution of these ten algebraic equations leads to

$$A = -\Delta'\beta^2\gamma^3\left\{150\alpha^3\beta t_1 - 3\Big[-2\alpha^5\beta t_2 + \left(15\alpha^4 + \alpha^6\right)t_3 + \alpha^3\beta t_4 - 45\alpha t_5 + \left(15 + 2\alpha^2\right)t_6\Big]\cosh(\beta - \alpha) + \Big[\left(15\alpha^4\beta + \alpha^6\beta\right)t_2 - 18\alpha^5 t_3 + \left(135 + 18\alpha^2\right)t_5 - 45\alpha t_6 - \alpha^3\left(t_6 + t_7\right)\Big]\sinh(\beta - \alpha)\right\}, \tag{A-24}$$

$$B = 5D_1\gamma^3, \tag{A-25}$$

$$C_1 = -\Delta'5\gamma^3\left\{30\alpha^3\left(\beta^3 + 2\gamma^3\right) + 3\Big[15\alpha^4\beta^2 + \alpha^6\beta^2 - 2\alpha^5\left(\beta^3 + 2\gamma^3\right) - 45\alpha t_8 - \alpha^3 t_9 + \left(15 + 2\alpha^2\right)t_{10}\Big]\cosh(\beta - \alpha) + \Big[18\alpha^5\beta^2 - \left(135 + 18\alpha^2\right)t_8 - \left(15\alpha^4 + \alpha^6\right)\left(\beta^3 + 2\gamma^3\right) + \alpha^3\left(45\beta^2 + t_{10}\right) + 45\alpha t_{10}\Big]\sinh(\beta - \alpha)\right\}, \tag{A-26}$$

$$C_3 = \Delta'15\gamma^3\left\{\left(\beta^3 - \gamma^3\right)t_{11} + 3\left(2\beta^3 + \gamma^3\right)t_{12}\cosh(\beta - \alpha) + 3\left(2\beta^3 + \gamma^3\right)t_{13}\sinh(\beta - \alpha)\right\}, \tag{A-27}$$

$$D_1 = \Delta'3\gamma^3\left\{t_{14}\cosh(\beta - \alpha) + t_{15}\sinh(\beta - \alpha)\right\}, \tag{A-28}$$

$$D_3 = \Delta'15\gamma^3\left\{\left(\beta^3 - \alpha^3\right)\left(\beta^3 - \gamma^3\right) - 3(\alpha - \beta)\left(\gamma^3 + 2\beta^3\right)\cosh(\beta - \alpha) + 3(\alpha\beta - 1)\left(\gamma^3 + 2\beta^3\right)\sinh(\beta - \alpha)\right\}, \tag{A-29}$$

$$E = \Delta'30\alpha^3\gamma^3\left\{10\beta^3\left(\beta^3 - \gamma^3\right) + \left(\gamma^3 + 2\beta^3\right)\left(t_{12} - \alpha^3 + \alpha^2\beta\right)\cosh(\beta - \alpha) + \left(\gamma^3 + 2\beta^3\right)\left(t_{13} - \alpha^2 + \alpha^3\beta\right)\sinh(\beta - \alpha)\right\}, \tag{A-30}$$

$$F = \Delta'15\gamma^3\left\{10\alpha^3\left(\beta^3 - \gamma^3\right) + \left(\gamma^3 + 2\beta^3\right)t_{16}\cosh(\beta - \alpha) + \left(\gamma^3 + 2\beta^3\right)t_{17}\sinh(\beta - \alpha)\right\}, \tag{A-31}$$

$$G = -\Delta'30\gamma^3\left\{-\alpha\left(\beta^3 - \gamma^3\right)t_{18}\cosh\alpha - 15\alpha^3\beta\left(\gamma^3 + 2\beta^3\right)\cosh\beta + 3\left(\beta^3 - \gamma^3\right)t_{19}\sinh\alpha + 15\alpha^3\left(\gamma^3 + 2\beta^3\right)\sinh\beta\right\}, \tag{A-32}$$

$$H = -\Delta'30\gamma^3\left\{-3\left(\beta^3 - \gamma^3\right)t_{19}\cosh\alpha - 15\alpha^3\left(\gamma^3 + 2\beta^3\right)\cosh\beta + \alpha\left(\beta^3 - \gamma^3\right)t_{18}\sinh\alpha + 15\alpha^3\beta\left(\gamma^3 + 2\beta^3\right)\sinh\beta\right\}, \tag{A-33}$$

where

$$\Delta' = \Big\{300\alpha^3 t_{20} + 3\Big[\left(30\alpha^4 + 2\alpha^6\right) t_{21} - 4\alpha^5 t_{22} - \alpha^3 t_{23} + \left(15 + 2\alpha^2\right) t_{24} - 45\alpha t_{25}\Big] \cosh(\beta - \alpha) + \Big[36\alpha^5 t_{21} - \left(30\alpha^4 + 2\alpha^6\right) t_{22} + 45\alpha t_{24} - \left(135 + 18\alpha^2\right) t_{25} - \alpha^3 t_{26}\Big] \sinh(\beta - \alpha)\Big\}^{-1}, \tag{A-34}$$

$$\begin{aligned}
t_1 &= \gamma^3 - 4\beta^3, \quad t_2 = 90\beta + 2\beta^3 - 5\gamma^3,\\
t_3 &= 30\beta + 4\beta^3 - 5\gamma^3, \quad t_4 = -450\beta - 20\beta^3 - 4\beta^5 + 35\gamma^3 + 5\beta^2\gamma^3\\
t_5 &= 10\beta^4 + 4\beta^6 - 10\beta\gamma^3 - 5\beta^3\gamma^3, \quad t_6 = 30\beta^5 + 2\beta^7 - 30\beta^2\gamma^3 - 5\beta^4\gamma^3,\\
t_7 &= 1350\beta + 180\beta^3 - 255\gamma^3, \quad t_8 = 2\beta^3 + \beta^5 + \gamma^3,\\
t_9 &= 7\beta^3 + \beta^5 + 11\gamma^3, \quad t_{10} = 6\beta^4 + \beta^6 + 3\beta\gamma^3 + 2\beta^3\gamma^3,\\
t_{11} &= \alpha^5 + 30\beta^3 - \alpha^2\beta^3, \quad t_{12} = 15\alpha + 2\alpha^3 - 15\beta - 7\alpha^2\beta,\\
t_{13} &= 15 + 7\alpha^2 - 15\alpha\beta - 2\alpha^3\beta,\\
t_{14} &= 15\alpha^4 + \alpha^6 - 6\alpha^5\beta - 45\alpha\beta^3 + 45\beta^4 + 6\alpha^2\beta^4 - \alpha^3\beta\left(15 + \beta^2\right),\\
t_{15} &= 6\alpha^5 - 15\alpha^4\beta - \alpha^6\beta - 45\beta^3 - 6\alpha^2\beta^3 + 45\alpha\beta^4 + \alpha^3\left(15 + \beta^4\right),\\
t_{16} &= 45\alpha + \alpha^3 - 45\beta - 6\alpha^2\beta, \quad t_{17} = 45 + 6\alpha^2 - 45\alpha\beta - \alpha^3\beta,\\
t_{18} &= 15\alpha^3 + \alpha^5 - 45\beta^3 - \alpha^2\beta^3, \quad t_{19} = 5\alpha^3 + 2\alpha^5 - 15\beta^3 - 2\alpha^2\beta^3,\\
t_{20} &= 2\beta^6 - \beta^3\gamma^3 - \gamma^6, \quad t_{21} = 15\beta^3 + 2\beta^5 - 5\beta^2\gamma^3 + 3\gamma^5,\\
t_{22} &= 45\beta^4 + \beta^6 - 5\beta^3\gamma^3 + 9\beta\gamma^5 - 5\gamma^6,\\
t_{23} &= 450\beta^4 + 20\beta^6 + 4\beta^8 - 10\beta^5\gamma^3 + 90\beta\gamma^5 - 55\gamma^6 + 2\beta^3\gamma^3\left(-35 + 3\gamma^5\right),\\
t_{24} &= 30\beta^7 + 2\beta^9 - 10\beta^6\gamma^3 - 15\beta\gamma^6 - 10\beta^3\gamma^6 + 6\beta^4\gamma^3\left(-10 + 3\gamma^2\right),\\
t_{25} &= 10\beta^6 + 4\beta^8 - 10\beta^5\gamma^3 - 5\gamma^6 + \beta^3\left(-20\gamma^3 + 6\gamma^5\right),\\
t_{26} &= -180\beta^5 - 30\beta^7 - 2\beta^9 + 450\beta^2\gamma^3 + 10\beta^6\gamma^3 - 270\gamma^5\\
&\quad + 15\beta\gamma^6 + \beta^4\left(60\gamma^3 - 18\gamma^5\right) + 10\beta^3\left(-135 + \gamma^6\right).
\end{aligned} \tag{A-35}$$

References

Bhatt, B.S., Sacheti, N.C.: Flow past a porous spherical shell using the Brinkman model. J. Phys. D Appl. Phys. **27**, 37–41 (1994). doi:10.1088/0022-3727/27/1/006

Brinkman, H.C.: A calculation of the viscous force exerted by a flowing fluid on a dense swarm of particles. Appl. Sci. Res. **A1**, 27–34 (1947)

Chen, S.B., Cai, A.: Hydrodynamic interactions and mean settling velocity of porous particles in a dilute suspension. J. Colloid Interface Sci. **217**, 328–340 (1999). doi:10.1006/jcis.1999.6353

Happel, J.: Viscous flow in multiparticle systems: slow motion of fluids relative to beds of spherical particles. AIChE J. **4**, 197–201 (1958). doi:10.1002/aic.690040214

Happel, J., Brenner, H.: Low Reynolds Number Hydrodynamics. Nijhoff, Dordrecht, The Netherlands (1983)

Jones, I.P.: Low Reynolds number flow past a porous spherical shell. Proc. Camb. Philos. Soc. **73**, 231–238 (1973). doi:10.1017/S0305004100047642

Keh, H.J., Chen, W.C.: Sedimentation velocity and potential in concentrated suspensions of charged porous spheres. J. Colloid Interface Sci. **296**, 710–720 (2006). doi:10.1016/j.jcis.2005.09.040

Keh, H.J., Chou, J.: Creeping motion of a composite sphere in a concentric spherical cavity. Chem. Eng. Sci. **59**, 407–415 (2004). doi:10.1016/j.ces.2003.10.006

Keh, H.J., Lu, Y.S.: Creeping motions of a porous spherical shell in a concentric spherical cavity. J. Fluids Struct. **20**, 735–747 (2005). doi:10.1016/j.jfluidstructs.2005.03.005

Koplik, J., Levine, H., Zee, A.: Viscosity renormalization in the Brinkman equation. Phys. Fluids **26**, 2864–2870 (1983). doi:10.1063/1.864050

Kuwabara, S.: The forces experienced by randomly distributed parallel circular cylinders or spheres in a viscous flow at small Reynolds numbers. J. Phys. Soc. Jpn. **14**, 527–532 (1959). doi:10.1143/JPSJ.14.527

Levine, S., Neale, G.H.: The prediction of electrokinetic phenomena within multiparticle systems I. Electrophoresis and electroosmosis. J. Colloid Interface Sci. **47**, 520–529 (1974). doi:10.1016/0021-9797(74)90284-7

Makino, K., Yamamoto, S., Fujimoto, K., Kawaguchi, H., Ohshima, H.: Surface structure of latex particles covered with temperature-sensitive hydrogel layers. J. Colloid Interface Sci. **166**, 251–258 (1994). doi:10.1006/jcis.1994.1291

Masliyah, J.H., Polikar, M.: Terminal velocity of porous spheres. Can. J. Chem. Eng. **58**, 299–302 (1980)

Masliyah, J.H., Neale, G., Malysa, K., van de Ven, T.G.M.: Creeping flow over a composite sphere: solid core with porous shell. Chem. Eng. Sci. **42**, 245–253 (1987). doi:10.1016/0009-2509(87)85054-6

Matsumoto, K., Suganuma, A.: Settling velocity of a permeable model floc. Chem. Eng. Sci. **32**, 445–447 (1977). doi:10.1016/0009-2509(77)85009-4

Neale, G., Epstein, N., Nader, W.: Creeping flow relative to permeable spheres. Chem. Eng. Sci. **28**, 1865–1874 (1973). doi:10.1016/0009-2509(73)85070-5

Ooms, G., Mijnlieff, P.F., Beckers, H.L.: Frictional force exerted by a flowing fluid on a permeable particle, with particular reference to polymer coils. J. Chem. Phys. **53**, 4123–4130 (1970). doi:10.1063/1.1673911

Prasad, D., Narayan, K.A., Chhabra, R.P.: Creeping fluid flow relative to an assemblage of composite spheres. Int. J. Eng. Sci. **28**, 215–230 (1990). doi:10.1016/0020-7225(90)90124-2

Qin, Y., Kaloni, P.N.: Creeping flow past a porous spherical shell. Z. Angew. Math. Mech. **73**, 77–84 (1993). doi:10.1002/zamm.19930730207

Simha, R.: A treatment of the viscosity of concentrated suspensions. J. Appl. Phys. **23**, 1020–1024 (1952). doi:10.1063/1.1702338

Srinivasacharya, D.: Motion of a porous sphere in a spherical container. C. R. Mecanique **333**, 612–616 (2005)

Stokes, G.G.: On the effect of the internal friction of fluid on pendulums. Trans. Camb. Philos. Soc. **9**, 8–106 (1851)

Sutherland, D.N., Tan, C.T.: Sedimentation of a porous sphere. Chem. Eng. Sci. **25**, 1948–1950 (1970). doi:10.1016/0009-2509(70)87013-0

Veerapaneni, S., Wiesner, M.R.: Hydrodynamics of fractal aggregates with radially varying permeability. J. Colloid Interface Sci. **177**, 45–57 (1996). doi:10.1006/jcis.1996.0005

Wei, Y.K., Keh, H.J.: Diffusiophoresis and electrophoresis in concentrated suspensions of charged colloidal spheres. Langmuir **17**, 1437–1447 (2001). doi:10.1021/la001387m